

Enhanced superconductivity in barium hydrides via light element incorporation

Yue-Wen Fang^{1, 2*} and Ion Errea^{1, 2, 3†}

¹ *Fisika Aplikatua Saila, Gipuzkoako Ingeniaritza Eskola,
University of the Basque Country (UPV/EHU),
Europa Plaza 1, 20018 Donostia/San Sebastián, Spain.*

² *Centro de Física de Materiales (CSIC-UPV/EHU),
Manuel de Lardizabal Pasealekua 5,
20018 Donostia/San Sebastián, Spain. and*

³ *Donostia International Physics Center (DIPC),
Manuel de Lardizabal Pasealekua 4,
20018 Donostia/San Sebastián, Spain.*

Abstract

Barium hydrides are of interest for their potential in both ionic conductivity and superconductivity. Recently, a superconducting hydride BaH_{12} containing H_2 and H_3^{-1} molecular units was experimentally reported with a critical temperature T_c of 20 K at 140 GPa. Herein, we combine ab initio methods with a rapid calculator of T_c based on the networking value model to predict that the introduction of light elements, such as Be, can effectively expand the structure diversity and structure space of barium hydrides. Although molecular hydrogen units are still widely present in thermodynamically stable and metastable crystal structures, we find that a metastable phase of BeBaH_8 shows a higher T_c of 49 K than BaH_{12} at a reduced pressure of 100 GPa. This BeBaH_8 remains dynamically stable at 15 GPa. Furthermore, our study shows that increasing pressure can further elevate T_c beyond 100 K by enhancing the electron-phonon coupling constant. Our study proposes a feasible method for broadening the structural landscape in the exploration of superconducting phases of barium hydrides.

* yuwen.fang@ehu.eus

† ion.errea@ehu.eus

1. INTRODUCTION

In recent years, the exploration of hydride has gained significant attention due to the pursuit of high critical temperature (T_c) superconductivity [1–3]. Both theoretical [4–9] and experimental studies [10–12] have suggested that high- T_c and even near room temperature superconductivity is possible in hydrides, despite the fact that the materials must be subject to an extremely high pressure, e.g. the clathrate superhydride LaH_{10} exhibits a T_c of around 250 K at 175 GPa [13–15]. Because the application of extremely high pressure favors isotropic properties, the experimentally observed high-pressure superconducting hydrides usually feature very high-symmetry structures [1, 16].

The neighbor of La in the periodic table, Ba, has been thought to be one of the promising host elements for the synthesis of superconducting hydrides [17]. At ambient pressure, the $Pnma$ BaH_2 ($\text{BaH}_2\text{-I}$) is the thermodynamical stable phase of barium hydride. Heating at ambient pressure can drive a structural transition of BaH_2 from the low-symmetry $Pnma$ to the high-symmetry Ni_2In -type structure with the space group $P6_3/mmc$ ($\text{BaH}_2\text{-II}$). This structure transition makes BaH_2 be one of the prominent ionic conductors with potential applications in energy storage because the high-symmetry phase exhibits a hydrogen ion conductivity of $0.2 \text{ S}\cdot\text{cm}^{-1}$ at 630°C that is an order of magnitude larger than that of state-of-the-art oxide ion conductors [18]. However, both $\text{BaH}_2\text{-I}$ and $\text{BaH}_2\text{-II}$ are not good candidates for superconductivity because they are semiconductors with a wide band gap around $1.9\sim 2.9 \text{ eV}$ [19]. The high-pressure experiments [20, 21] suggest that BaH_2 undergoes successive phase transformations: $\text{BaH}_2\text{-I}$ first converts to $\text{BaH}_2\text{-II}$ at around 2.5 GPa, then transforms to AlB_2 -type simple hexagonal $\text{BaH}_2\text{-III}$ accompanied by a closure of the band gap at around 57 GPa. Although $\text{BaH}_2\text{-III}$ is metallic, superconductivity has not been observed.

Chen et al studied barium hydrides at higher pressures ranging from 75 to 173 GPa and reported several hydrogen-rich barium hydrides [17]. In particular, their transport measurements revealed the onset of superconductivity at 20 K and 140 GPa in BaH_{12} with a pseudocubic face-centered cubic Ba sublattice. This superconducting hydride is suggested to be a unique molecular hydride because it contains H_2 and H_3^{-1} molecular units, forming separate flat H_{12} chains, which are rarely observed in the high-symmetry clathrate superhydrides at high pressures. In hydrides with H_2 and H_3^{-1} molecular units, the H-H bond

disrupts the delocalized metallic bonding network, and their covalent nature may reduce the interaction between the vibrational modes of hydrogen atoms and the electronic states of the host lattice, which can lead to weaker electron-phonon coupling. Several recent studies have shown that the presence of hydrogen molecules generally form more insulating states than metallic states [4, 22]. Therefore, the molecular hydrogen units are generally not beneficial for superconductivity and high T_c .

Based on the networking value model and the statistics of hundreds of superconducting hydrides, an earlier study by one of the authors suggests that stretching the H-H bond or elimination of the hydrogen molecular units can favor superconductivity [16]. Guided by this quantitative rule, in our study, we design new ternary barium hydrides that show higher T_c than BaH_{12} at lower pressures. Aiming at eliminating or reducing the number of H_2 and H_3^{-1} molecular units in barium hydride, we introduce four elements with light atomic mass (Li, Be, B and C) to barium hydride and perform high-throughput crystal structure screening to locate the low-enthalpy structures up to 200 GPa. By studying the structural and electronic properties of a series of low-lying ternary barium hydride, we find that H_2 molecular units remain widely observed in these ternary barium hydrides, while H_3^{-1} is almost absent. Due to the universal existence of molecular units in the studied ternary hydrides, more insulating states than metallic states are found in the low-enthalpy structure space. Although metallic states were much fewer than the semiconducting or insulating phases, there are several metallic molecular hydrides showing interesting properties. In particular, BeBaH_4 with tetragonal structure is nearly thermodynamically stable at 100 GPa and can be still dynamically stable at 50 GPa. In addition, by combining the quick estimator of superconducting T_c based on the networking value model [16, 23] with the ab initio methods, BeBaH_8 with orthorhombic structure has been predicted to be superconducting with a T_c of 49 K at 100 GPa. The value of T_c can be further boosted by improving the pressure, reaching 107 K at 200 GPa. This BeBaH_8 remains dynamically stable down to 15 GPa although it is not superconducting due to the substantial reduction of the electron-phonon coupling constant.

2. METHODS

2.1. Crystal structure prediction

The crystal structure prediction methods, i.e., the particle swarm algorithm implemented in CALYPSO [24, 25] and the evolutionary algorithm implemented in CrySPY [26], were used to predict the crystal structures of A -Ba-H ($A = \text{Li, Be, B and C}$) at pressures up to 200 GPa. The crystal structure prediction was performed with a fixed composition, and cell sizes were explored up to 32 atoms per cell. A total of around 100,000 structures were screened during the crystal structure prediction. The enthalpy and forces of the predicted crystal structures were calculated by first-principles density functional theory (DFT) methods. The DFT calculations were carried out using the Vienna Ab initio Simulation Package (VASP) [27, 28] employing the projector-augmented wave (PAW) method. The exchange-correlation functional was treated in the generalized gradient approximation within the parameterization of Perdew, Burke, and Ernzerhof [29]. To generate k -points for different crystal structures during structure screening, we employed the k -point generation scheme in Pymatgen [30], using a grid density of 100 k -points per \AA^{-3} of reciprocal cell volume. An energy cutoff of 450 eV was used in the crystal structure prediction. To construct the convex hull phase diagram, we considered all materials available in our crystal structure prediction, as well as those we could find from the Materials Project [31]. The structures were fully optimized until the energy convergence criterion of 10^{-8} eV and force criterion of 10^{-3} eV $\cdot\text{\AA}^{-1}$ were satisfied.

2.2. Electronic structure calculations

In high-throughput DFT calculations of the density of states (DOS), we used the Gaussian smearing method in VASP. To ensure accurate results, we used a narrow smearing width of 0.05 eV accompanied by a dense k point grid with 200 points per \AA^{-3} of reciprocal cell volume. To extract the total DOS and the element/orbital projected DOS, we used the Sumo [32] code. In both band and phonon dispersion calculations, the special k -path were generated using Sumo [32]. To estimate the superconducting critical temperature T_c based on the networking value model, we used the TcESTIME code [16, 23]. The value of T_c with

an error of 60 K is correlated to Φ_{DOS} :

$$T_c = (750\Phi_{\text{DOS}} - 85) \text{ K}, \quad (1)$$

$$\Phi_{\text{DOS}} = \phi H_f H_{\text{DOS}}^{-3} \quad (2)$$

where ϕ is the networking value based on the electron localization function, H_f is the hydrogen fraction, and H_{DOS} is the hydrogen fraction of the total DOS at the Fermi energy.

2.3. Phonon and electron-phonon coupling calculations

The phonon, and electron-phonon coupling properties were investigated using density-functional perturbation theory (DFPT) method implemented in Quantum Espresso [33, 34]. The dynamical stability was also cross-checked by the supercell and finite displacement methods implemented in Phonopy [35]. The Quantum Espresso calculations were performed using norm-conserving pseudopotentials from the strict set of PseudoDojo [36]. In Quantum Espresso calculations, geometry optimizations were carried out using uniform Γ -centered k -point grids with a density of 3000 k -points. In the electron-phonon coupling calculations, the k -grid from the structure relaxation was doubled in each direction as the coarse grid. In addition, and it was further quadrupled in each direction as the fine grid. In the particular case of BeBaH₈, the results converged well with a k -grid of $42 \times 42 \times 42$. The critical temperature for superconductivity was calculated using the Allen-Dynes formula:

$$T_c = \frac{f_1 f_2 \omega_{\log}}{1.20} \exp\left(\frac{-1.04(1 + \lambda)}{\lambda - \mu^*(1 + 0.62\lambda)}\right), \quad (3)$$

$$f_1 = \left(1 + \left(\frac{\lambda}{2.46(1 + 3.8\mu^*)}\right)^{3/2}\right)^{1/3}, \quad (4)$$

$$f_2 = \left(1 + \frac{\lambda^2 \left(\frac{\bar{\omega}_2}{\omega_{\log}} - 1\right)}{\lambda^2 + [1.82(1 + 6.3\mu^*)\left(\frac{\bar{\omega}_2}{\omega_{\log}}\right)]^2}\right), \quad (5)$$

where f_1 and f_2 are correction factor depending on the electron-coupling constant λ , Coulomb pseudopotential parameter μ^* , average logarithm frequency ω_{\log} , and $\bar{\omega}_2$. The frequencies $\bar{\omega}_n$ are the n^{th} root of the n^{th} moment of the normalized distribution $g(\omega) = \frac{2}{\lambda\omega} \alpha^2 F(\omega)$ [37]. In our study, the Coulomb pseudopotential parameter (μ^*) of 0.1 was used.

3. RESULTS

3.1. $A_2\text{BaH}_{12}$ at 200 GPa where $A = \text{Li, Be, B, and C}$

Chen *et al.* reported the molecular hydride BaH_{12} exhibited a T_c of 20 K at 140 GPa experimentally [17]. To investigate the effect of the introduced light-mass elements ($A = \text{Li, Be, B, and C}$) on BaH_{12} at high pressures, we first performed crystal structure prediction of 2 formula units $A_2\text{BaH}_{12}$ (i.e. 30-atom $A_4\text{Ba}_2\text{H}_{24}$) at 200 GPa. In each crystal structure prediction, we carried out around 20-50 generations for each fixed stoichiometry, with each generation including 100 crystal structures. For each stoichiometry of $A_2\text{BaH}_{12}$, the structural and electronic properties of the twenty low-lying states are studied. The space group and enthalpy of the low-lying structures for LiBaH_{12} , BeBaH_{12} , BBaH_{12} and CBaH_{12} are shown in Supplementary Table 1, Table 2, Table 3 and Table 4, respectively. The crystal structures of the lowest-enthalpy states at 200 GPa, as predicted by our crystal structure calculations, are shown in Figure 1.

Because the 2 f.u. $A_2\text{BaH}_{12}$ is a large cell and most predicted structures show low symmetry (most of them being $P1$ without any symmetry operation except identity operation), it is computationally demanding to carry out an high-throughput calculation of T_c using DFPT methods implemented in Quantum Espresso. Alternatively, we note that the networking value model [16, 23] has been widely recognized and used in many recent studies to predict superconducting critical temperatures [38–40]. Because the networking value model is based on electron localization functions that can be obtained in standard ab initio calculations, it makes the estimation of T_c much computationally cheaper compared to the direct computation from solving Eliashberg spectral functions in DFPT calculations. Previously, the networking value model was applied into the high-throughput calculation of T_c and guided the theoretical discovery of the 100 K superconductivity in $\text{Lu}_4\text{H}_{11}\text{N}$ and the near-room-temperature superconductivity in binary LuH_6 and LuH_{10} [4].

By using the networking value model method implemented in TcESTIME [16], we calculated the critical temperatures for the low-lying metallic structures of the 30-atom $A_2\text{BaH}_{12}$ at 200 GPa. The values obtained are shown in the Supplementary Tables 1~4. The highest T_c for $\text{Li}_2\text{BaH}_{12}$ is 56 K while no superconducting phase is observed in $\text{C}_2\text{BaH}_{12}$. Both BeBaH_{12} and BBaH_{12} show critical temperatures above 70 K which approach the boiling point

of liquid nitrogen.

In examining B_2BaH_{12} and C_2BaH_{12} , we note from Supplementary Tables 1–4 that more than half of the structures among the twenty low-enthalpy states exhibit insulating character. Relatively, more low-lying structures of Li_2BaH_{12} and Be_2BaH_{12} show metallic conductivity. The analysis of these low-lying structures of $ABaH_{12}$ at 200 GPa demonstrates that the introduction of Li and Be into the barium hydrides has more possibilities to form metallic properties than B and C. In particular, the lowest-lying structures of $P4bm$ B_2BaH_{12} and $P1$ C_2BaH_{12} , illustrated in in Figure 1 are both insulating, whereas the lowest-lying states of Cc Li_2BaH_{12} and $Cmmm$ Be_2BaH_{12} are both metallic. Although the lowest-lying structures of Li_2BaH_{12} and Be_2BaH_{12} are metals, the minimal interatomic distances in Table I show that their minimal H-H bond lengths are 0.830 and 0.756 Å, respectively, which is just slightly larger than the minimal H-H bond lengths in B_2BaH_{12} and C_2BaH_{12} . Therefore, the H_2 molecule units are present in all the ground-state structures of $ABaH_{12}$ (see Figure 1). However, unlike the other three cases but like the $Cmc2_1$ BaH_{12} reported by Chen et al [17], the H-H-H (H_3^{-1}) chain is only observed in Li_2BaH_{12} , as illustrated in Figure 1(a).

TABLE I. The minimal interatomic distances in the lowest-enthalpy states of $ABaH_{12}$ at 200 GPa, where $A = Li, Be, B,$ and C .

Element	A H-H (Å)	A-H (Å)	A-A (Å)	Ba-H (Å)
Li	0.830	1.402	1.855	1.971
Be	0.756	1.350	4.011	2.066
B	0.741	1.100	3.108	2.069
C	0.747	1.046	1.377	1.975

3.2. $BeBaH_x$ at pressures

Given that the analysis at 200 GPa indicates that the incorporation of Be and Li into Ba-H promotes the formation of more metallic states compared to B and C, and that T_c is expected to be higher for Be than for Li, we further investigated $BeBaH_x$ ($x = 2n, n \in \{1, 2, 3, \dots, 12\}$). However, we shifted our focus to explore the structures at 100 GPa to identify potential superconducting Be-Ba-H compounds that could be stabilized at pressures lower than those experimentally reported for barium hydrides. [17]. Figure 2 shows

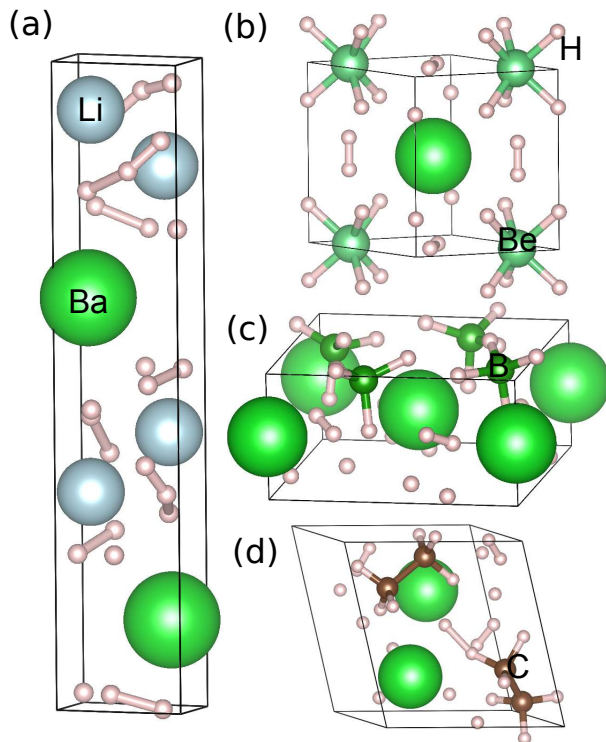


FIG. 1. The lowest-lying states at 200 GPa of (a) $\text{Li}_2\text{BaH}_{12}$ with space group Cc , (b) $\text{Be}_2\text{BaH}_{12}$ with space group $Cmmm$, (c) $\text{B}_2\text{BaH}_{12}$ with space group $P4bm$, and (d) $\text{C}_2\text{BaH}_{12}$ with $P1$. The H-H bond is plotted if the distances are less than 1.0 \AA , A-A and A-H bonds are plotted if the distances are less than 1.4 \AA .

the phase diagram at 100 GPa based on the crystal structures from our crystal structure prediction and Materials Project database [31]. We find the BeBaH_6 and BeBaH_{18} are on the convex hull, which implies that they are thermodynamically stable. However, they are both semiconductors.

Although we did not find any thermodynamically stable BeBaH_x compounds that are metallic, we identified several metallic stoichiometries lying within 100 meV/atom from the convex hull. In particular, by estimating T_c using the networking value model, we find that two hydrides, BeBaH_4 and BeBaH_8 , may be superconducting with T_c higher than 25 K (± 60 K). These two hydrides BeBaH_4 and BeBaH_8 are 11 meV/atom and 36 meV/atom above the convex hull, respectively at 100 GPa. Since these two compounds are not far from the convex hull, implying the feasibility of experimental synthesis, the electron-phonon coupling properties of these two structures were further investigated using DFPT method.

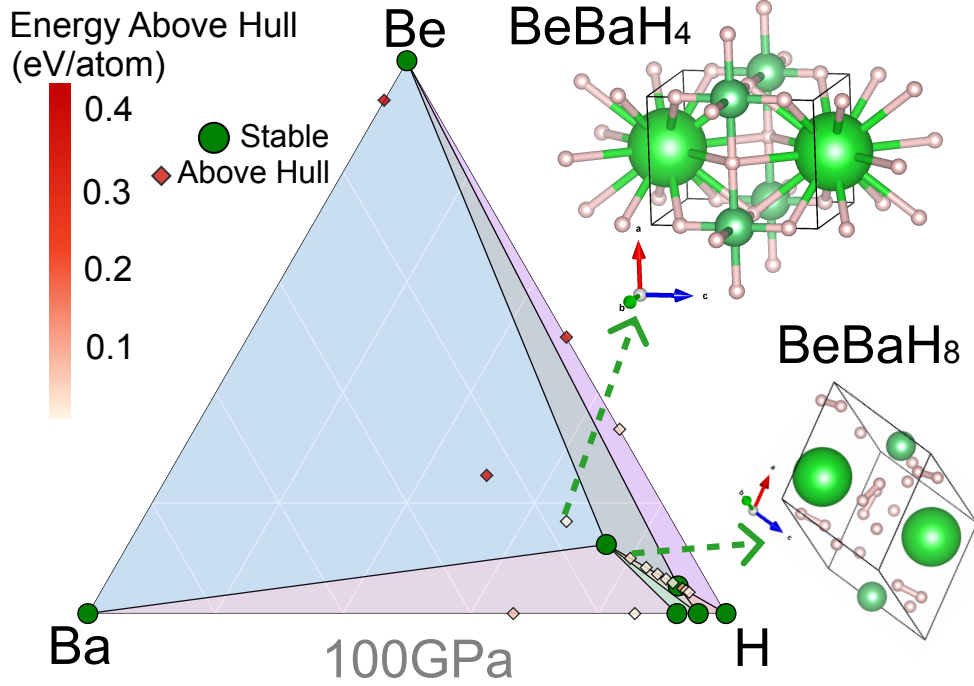


FIG. 2. The phase diagram at 100 GPa and the crystal structures of two metastable phases BeBaH₄ and BeBaH₈.

The hydride BeBaH₄ has a tetragonal crystal structure and a space group of $P4/mmm$ (No. 123) at 100 GPa, in which $a = 2.91 \text{ \AA}$ and $c = 3.87 \text{ \AA}$. The crystal structure is shown in Fig. 2. At 100 GPa, the phonon spectrum in Fig. 3 shows that this $P4/mmm$ BeBaH₄ is dynamically stable. However, because of the small electron-phonon coupling constant λ of 0.15, the Allen-Dynes formula predicts that it is not a superconductor at 100 GPa. We find that a higher pressure of 200 GPa does not help to develop superconductivity because the value of λ is only slightly increased to 0.16. Despite the absence of superconductivity, this tetragonal BeBaH₄ can be stabilized at a lower pressure of 50 GPa. By comparing the phonon spectra at 50 and 100 GPa, we can find that the decreased pressure only has a small effect on the low-energy phonon modes consisting of heavy atoms Be and Ba, but in the meantime it softens the high-energy hydrogen modes significantly.

The crystal structure of BeBaH₈ has an orthorhombic Bravais lattice and a space group of $Cmc2_1$ (No. 36). There are two formula units in the primitive cell, resulting in 20 atoms in the primitive cell. The primitive cell of BeBaH₈ is shown schematically in Fig. 2. At 100 GPa, the electronic band structure and the density of states in Fig. 4 suggest that BeBaH₈ is metallically conductive. There are two bands crossing the Fermi level, forming

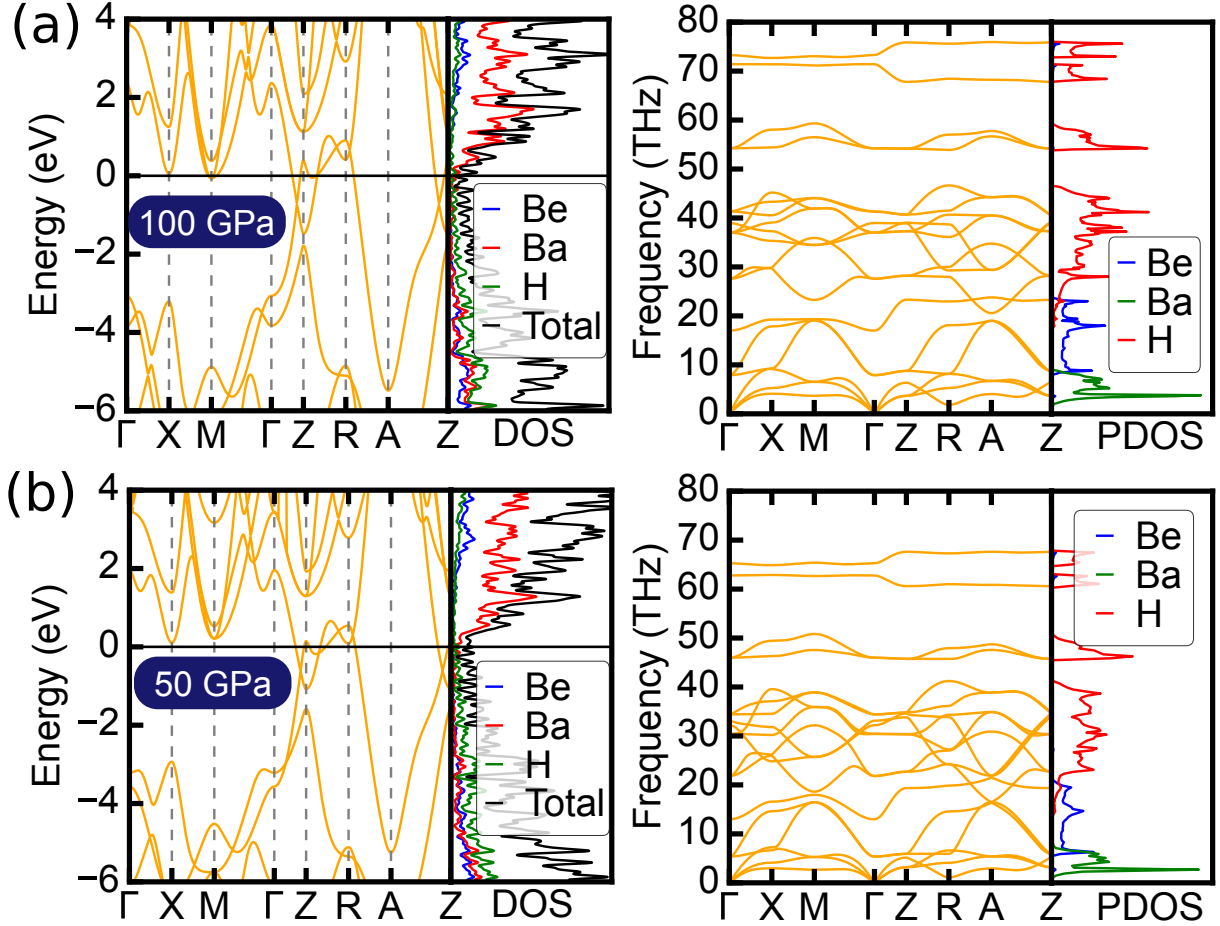


FIG. 3. The electronic and phonon properties of BeBaH_4 at 100 and 50 GPa. (a) Electronic band structure, electronic density of states (DOS), phonon band structure and phonon density of states (PDOS) at 100 GPa. (b) Electronic band structure, DOS, phonon band structure and PDOS at 50 GPa.

one electron pocket at Y and one hole pocket at Γ . More importantly, the electronic states at the Fermi level are dominated by hydrogen atoms with minor contributions from the heavy host metals Ba and Be, signaling that BeBaH_8 may be a hydride superconductor. The phonon dispersions and phonon density of states (PDOS) do not show any imaginary mode, indicating that BeBaH_8 is dynamically stable at 100 GPa. Furthermore, we find that BeBaH_8 remains dynamically stable in the harmonic approximation at pressures down to only 15 GPa, as evidenced by the phonon bands and PDOS shown in Fig. 4(b). However, the electronic band structure and DOS in Fig. 4(b) show that BeBaH_8 enters into the semiconducting state, exhibiting an indirect band gap of 1.5 eV.

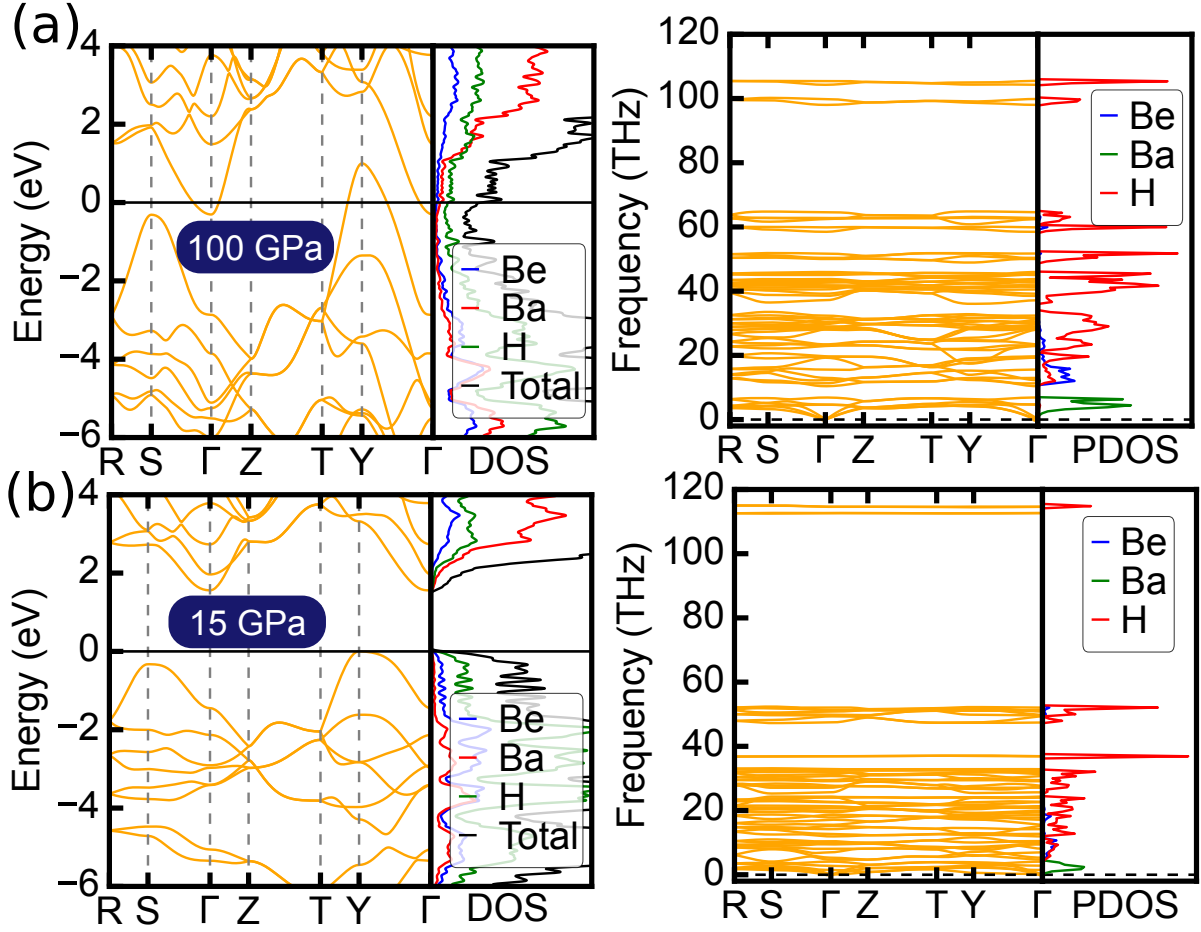


FIG. 4. The electronic and phonon properties of BeBaH₈ at 100 and 15 GPa. (a) Electronic band structure, electronic density of states (DOS), phonon band structure and phonon density of states (PDOS) at 100 GPa. (b) Electronic band structure, DOS, phonon band structure and PDOS at 15 GPa.

By solving the Eliashberg spectral function $\alpha^2F(\omega)$, the electron-phonon coupling constant of BeBaH₈ is calculated to be around 0.8 at 100 GPa. The corresponding Eliashberg spectral function $\alpha^2F(\omega)$ and the cumulative frequency-dependent electron-phonon function $\lambda(\omega)$ are shown in Fig. 5. By comparing the $\alpha^2F(\omega)$ and the phonon density of states in Fig. 4, we find that the electron-phonon coupling is dominated by the phonon modes of H and Be character ranging from 10 THz to 40 THz, followed by the minor contribution of phonon modes of Ba below 10 THz. Using Allen-Dynes equation with Coulomb pseudopotential parameter (μ^*) of a typical value 0.1, the value of T_c is around 49 K. Upon increasing pressure, we find that the electron-phonon coupling can be enhanced significantly. The Eliashberg

spectral functions $\alpha^2F(\omega)$ of 150 GPa and 200 GPa are compared to that at 100 GPa in Fig. 5. Due to the overall softening of the high-frequency pure H modes, these modes join to contribute additional electron-phonon coupling at 150 and 200 GPa, compared to the case of 100 GPa in which the high-frequency pure H modes almost have negligible contributions to λ . As a result, the values of T_c are increased to 73 K and 107 K at 150 GPa and 200 GPa, respectively.

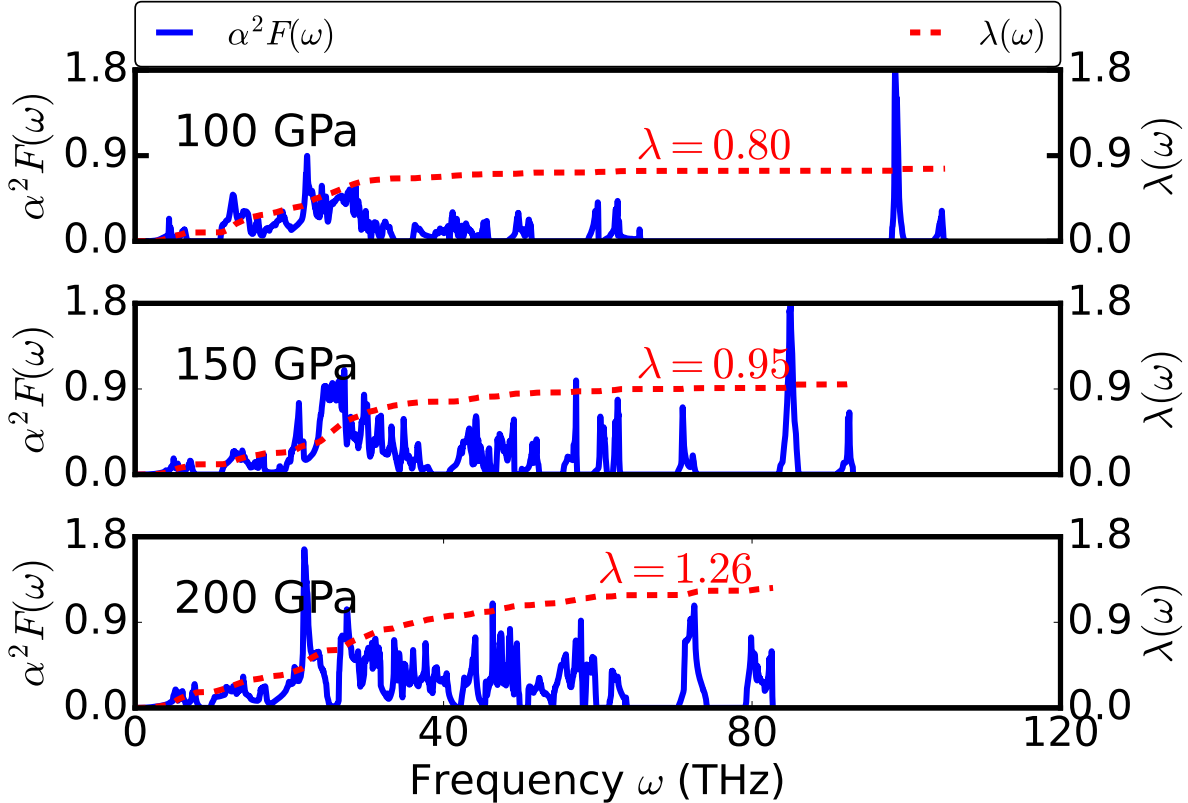


FIG. 5. Eliashberg spectral function $\alpha^2F(\omega)$ (solid blue lines) and the cumulative frequency-dependent electron-phonon coupling function $\lambda(\omega)$ (dashed red lines) of BeBaH₈ at 100, 150 and 200 GPa.

4. DISCUSSION & CONCLUSIONS

By combining the quick estimator of superconducting T_c with the high-throughput first-principles structure screening, we explore the possibility of implementation of superconductivity in the ternary barium hydrides A -Ba-H ($A = \text{Li, Be, B and C}$). Although the

introduction of these four light elements into barium hydrides does not eliminate the H_2 or H_3^{-1} molecular units completely in the low-lying structure space, they have significantly changed the low-lying crystal structures compared to those in Ba-H. Compared to the molecular hydrides BaH_{12} with T_c of 20 K at 140 GPa, we have predicted higher superconducting T_c of 49 K in BeBaH_8 at a reduced pressure of 100 GPa. The superconductivity in BeBaH_8 is effectively modulated by pressure, as the electron-phonon coupling constant is strongly affected by pressure. At higher pressures, such as 200 GPa, the critical temperature T_c reaches 107 K, while at lower pressures around 15 GPa, superconductivity vanishes with the band gap opening. Our study demonstrates a method to expand the structural space of barium hydrides by incorporating light elements, thereby enhancing the T_c of superconducting barium hydrides at reduced pressures. This approach is expected to stimulate further research efforts in synthesis and experimental measurements of barium hydrides, and will be applicable to design other moderate or ambient pressure hydride superconductors.

DECLARATIONS

Acknowledgments

This work is supported by the European Research Council (ERC) under the European Unions Horizon 2020 research and innovation program (Grant Agreement No. 802533), the Spanish Ministry of Science and Innovation (Grant No. PID2022142861NA-I00), the Department of Education, Universities and Research of the Eusko Jaurlaritza and the University of the Basque Country UPV/EHU (Grant No. IT1527-22), and Simons Foundation through the Collaboration on New Frontiers in Superconductivity. We acknowledge EuroHPC for granting us access to Lumi located in CSC's data center in Kajaani, Finland, (Project ID EHPC-REG-2024R01-084) and to RES for giving us access to MareNostrum5, Spain, (Project ID FI-2024-2-0035). Technical and human support provided by DIPC Supercomputing Center is gratefully acknowledged. The authors acknowledge enlightening discussions with the partners of the SuperC collaboration. Thanks also go to Wuhao Chen and Dmitrii V. Semenov for the helpful discussions.

Authors' contributions

Both Y.-W.F. and I.E. designed this project and wrote this manuscript. Y.-W.F. performed the calculations.

Availability of data and materials

The data supporting the findings can be found within the manuscript.

Conflicts of interest

All authors declared that there are no conflicts of interest.

-
- [1] B. Lilia, R. Hennig, P. Hirschfeld, G. Profeta, A. Sanna, E. Zurek, W. E. Pickett, M. Amsler, R. Dias, M. I. Erements, C. Heil, R. J. Hemley, H. Liu, Y. Ma, C. Pierleoni, A. N. Kolmogorov, N. Rybin, D. Novoselov, V. Anisimov, A. R. Oganov, C. J. Pickard, T. Bi, R. Arita, I. Errea, C. Pellegrini, R. Requist, E. K. U. Gross, E. R. Margine, S. R. Xie, Y. Quan, A. Hire, L. Fanfarillo, G. R. Stewart, J. J. Hamlin, V. Stanev, R. S. Gonnelli, E. Piatti, D. Romanin, D. Daghero, and R. Valenti, The 2021 room-temperature superconductivity roadmap, *Journal of Physics: Condensed Matter* **34**, 183002 (2022).
 - [2] W. Zhao, X. Huang, Z. Zhang, S. Chen, M. Du, D. Duan, and T. Cui, Superconducting ternary hydrides: progress and challenges, *National Science Review* **11**, nwad307 (2023), <https://academic.oup.com/nsr/article-pdf/11/7/nwad307/58227815/nwad307.pdf>.
 - [3] Y. Sun, X. Zhong, H. Liu, and Y. Ma, Clathrate metal superhydrides under high-pressure conditions: enroute to room-temperature superconductivity, *National Science Review* **11**, nwad270 (2023).
 - [4] Y.-W. Fang, Đorđe Dangić, and I. Errea, Assessing the feasibility of near-ambient conditions superconductivity in the lu-n-h system (2023), arXiv:2307.10699 [cond-mat.supr-con].
 - [5] Y. Sun, J. Lv, Y. Xie, H. Liu, and Y. Ma, Route to a superconducting phase above room temperature in electron-doped hydride compounds under high pressure, *Phys. Rev. Lett.* **123**, 097001 (2019).

- [6] I. Errea, F. Belli, L. Monacelli, A. Sanna, T. Koretsune, T. Tadano, R. Bianco, M. Calandra, R. Arita, F. Mauri, and J. A. Flores-Livas, Quantum crystal structure in the 250-kelvin superconducting lanthanum hydride, *Nature* **578**, 66 (2020).
- [7] G. M. Shutov, D. V. Semenov, I. A. Kruglov, and A. R. Oganov, Ternary superconducting hydrides in the la–mg–h system, *Materials Today Physics* **40**, 101300 (2024).
- [8] S. Saha, S. Di Cataldo, F. Giannessi, A. Cucciari, W. von der Linden, and L. Boeri, Mapping superconductivity in high-pressure hydrides: The superhydra project, *Phys. Rev. Mater.* **7**, 054806 (2023).
- [9] D. Duan, Y. Liu, F. Tian, D. Li, X. Huang, Z. Zhao, H. Yu, B. Liu, W. Tian, and T. Cui, Pressure-induced metallization of dense (h₂s)₂h₂ with high-*t_c* superconductivity, *Sci Rep* **4**, 3150 (2015).
- [10] A. P. Drozdov, M. I. Eremets, I. A. Troyan, V. Ksenofontov, and S. I. Shylin, Conventional superconductivity at 203 kelvin at high pressures in the sulfur hydride system, *Nature* **525**, 73 (2015).
- [11] Y. Song, J. Bi, Y. Nakamoto, K. Shimizu, H. Liu, B. Zou, G. Liu, H. Wang, and Y. Ma, Stoichiometric ternary superhydride labe_{h8} as a new template for high-temperature superconductivity at 110 k under 80 gpa, *Phys. Rev. Lett.* **130**, 266001 (2023).
- [12] I. A. Troyan, D. V. Semenov, A. G. Kvashnin, A. V. Sadakov, O. A. Sobolevskiy, V. M. Pudalov, A. G. Ivanova, V. B. Prakapenka, E. Greenberg, A. G. Gavriliuk, I. S. Lyubutin, V. V. Struzhkin, A. Bergara, I. Errea, R. Bianco, M. Calandra, F. Mauri, L. Monacelli, R. Akashi, and A. R. Oganov, Anomalous high-temperature superconductivity in yh₆, *Adv. Mater.* **33**, 2006832 (2021).
- [13] M. Somayazulu, M. Ahart, A. K. Mishra, Z. M. Geballe, M. Baldini, Y. Meng, V. V. Struzhkin, and R. J. Hemley, Evidence for superconductivity above 260 k in lanthanum superhydride at megabar pressures, *Phys. Rev. Lett.* **122**, 027001 (2019).
- [14] A. P. Drozdov, P. P. Kong, V. S. Minkov, S. P. Besedin, M. A. Kuzovnikov, S. Mozaffari, L. Balicas, F. F. Balakirev, D. E. Graf, V. B. Prakapenka, E. Greenberg, D. A. Knyazev, M. Tkacz, and M. I. Eremets, Superconductivity at 250 k in lanthanum hydride under high pressures, *Nature* **569**, 528 (2019).
- [15] H. Liu, I. I. Naumov, R. Hoffmann, N. W. Ashcroft, and R. J. Hemley, Potential high-*T_c* superconducting lanthanum and yttrium hydrides at high pressure, *Proc. Natl. Acad. Sci.*

- U.S.A. **114**, 6990 (2017).
- [16] F. Belli, T. Novoa, J. Contreras-García, and I. Errea, Strong correlation between electronic bonding network and critical temperature in hydrogen-based superconductors, *Nat Commun* **12**, 1748 (2021).
- [17] W. Chen, D. V. Semenok, A. G. Kvashnin, X. Huang, I. A. Kruglov, M. Galasso, H. Song, D. Duan, A. F. Goncharov, V. B. Prakapenka, A. R. Oganov, and T. Cui, Synthesis of molecular metallic barium superhydride: pseudocubic bah₁₂, *Nat Commun* **12**, 331 (2021).
- [18] M. C. Verbraeken, C. Cheung, E. Suard, and J. T. S. Irvine, High h⁻ ionic conductivity in barium hydride, *Nature Mater* **14**, 95 (2015).
- [19] W. Luo and R. Ahuja, Ab initio prediction of high-pressure structural phase transition in bah₂, *Journal of Alloys and Compounds* **446-447**, 405 (2007), proceedings of the International Symposium on Metal-Hydrogen Systems, Fundamentals and Applications (MH2006).
- [20] K. Kinoshita, M. Nishimura, Y. Akahama, and H. Kawamura, Pressure-induced phase transition of bah₂ : Post ni₂in phase, *Solid State Communications* **141**, 69 (2007).
- [21] H. A. Shuttleworth, I. Osmond, C. Strain, J. Binns, J. Buhot, S. Friedemann, R. T. Howie, E. Gregoryanz, and M. Peña Alvarez, Pressure-induced metallization of bah₂ and the effect of hydrogenation, *J. Phys. Chem. Lett.* **14**, 11490 (2023).
- [22] P. P. Ferreira, L. J. Conway, A. Cucciari, S. Di Cataldo, F. Giannessi, E. Kogler, L. T. F. Eleno, C. J. Pickard, C. Heil, and L. Boeri, Search for ambient superconductivity in the lu-n-h system, *Nat Commun* **14**, 244 (2023).
- [23] T. Novoa, M. E. di Mauro, D. Inostroza, K. El Haloui, N. Sisourat, Y. Maday, and J. Contreras-García, Tcestime: predicting high-temperature hydrogen-based superconductors, *Chem. Sci.* , (2024).
- [24] Y. Wang, J. Lv, L. Zhu, and Y. Ma, Crystal structure prediction via particle-swarm optimization, *Phys. Rev. B* **82**, 094116 (2010).
- [25] Y. Wang, J. Lv, L. Zhu, and Y. Ma, Calypso: A method for crystal structure prediction, *Computer Physics Communications* **183**, 2063 (2012).
- [26] T. Yamashita, S. Kanehira, N. Sato, H. Kino, K. Terayama, H. Sawahata, T. Sato, F. Utsuno, K. Tsuda, T. Miyake, and T. Oguchi, Cryspy: a crystal structure prediction tool accelerated by machine learning, *Science and Technology of Advanced Materials: Methods* **1**, 87 (2021).

- [27] G. Kresse and J. Furthmüller, Efficient iterative schemes for ab initio total-energy calculations using a plane-wave basis set, *Phys. Rev. B* **54**, 11169 (1996).
- [28] G. Kresse and J. Furthmüller, Efficiency of ab-initio total energy calculations for metals and semiconductors using a plane-wave basis set, *Computational Materials Science* **6**, 15 (1996).
- [29] J. P. Perdew, K. Burke, and M. Ernzerhof, Generalized gradient approximation made simple, *Phys. Rev. Lett.* **77**, 3865 (1996).
- [30] A. Jain, G. Hautier, C. J. Moore, S. Ping Ong, C. C. Fischer, T. Mueller, K. A. Persson, and G. Ceder, A high-throughput infrastructure for density functional theory calculations, *Computational Materials Science* **50**, 2295 (2011).
- [31] A. Jain, S. P. Ong, G. Hautier, W. Chen, W. D. Richards, S. Dacek, S. Cholia, D. Gunter, D. Skinner, G. Ceder, and K. A. Persson, Commentary: The materials project: A materials genome approach to accelerating materials innovation, *APL Materials* **1**, 011002 (2013).
- [32] A. M. Ganose, A. J. Jackson, and D. O. Scanlon, sumo: Command-line tools for plotting and analysis of periodic *ab initio* calculations, *Journal of Open Source Software* **3**, 717 (2018).
- [33] P. Giannozzi, S. Baroni, N. Bonini, M. Calandra, R. Car, C. Cavazzoni, D. Ceresoli, G. L. Chiarotti, M. Cococcioni, I. Dabo, A. Dal Corso, S. de Gironcoli, S. Fabris, G. Fratesi, R. Gebauer, U. Gerstmann, C. Gougoussis, A. Kokalj, M. Lazzeri, L. Martin-Samos, N. Marzari, F. Mauri, R. Mazzarello, S. Paolini, A. Pasquarello, L. Paulatto, C. Sbraccia, S. Scandolo, G. Scaluzero, A. P. Seitsonen, A. Smogunov, P. Umari, and R. M. Wentzcovitch, Quantum espresso: a modular and open-source software project for quantum simulations of materials, *Journal of Physics: Condensed Matter* **21**, 395502 (19pp) (2009).
- [34] P. Giannozzi, O. Andreussi, T. Brumme, O. Bunau, M. B. Nardelli, M. Calandra, R. Car, C. Cavazzoni, D. Ceresoli, M. Cococcioni, N. Colonna, I. Carnimeo, A. D. Corso, S. de Gironcoli, P. Delugas, R. A. D. Jr, A. Ferretti, A. Floris, G. Fratesi, G. Fugallo, R. Gebauer, U. Gerstmann, F. Giustino, T. Gorni, J. Jia, M. Kawamura, H.-Y. Ko, A. Kokalj, E. Küçükbenli, M. Lazzeri, M. Marsili, N. Marzari, F. Mauri, N. L. Nguyen, H.-V. Nguyen, A. O. de-la Roza, L. Paulatto, S. Poncé, D. Rocca, R. Sabatini, B. Santra, M. Schlipf, A. P. Seitsonen, A. Smogunov, I. Timrov, T. Thonhauser, P. Umari, N. Vast, X. Wu, and S. Baroni, Advanced capabilities for materials modelling with quantum espresso, *Journal of Physics: Condensed Matter* **29**, 465901 (2017).

- [35] A. Togo and I. Tanaka, First principles phonon calculations in materials science, *Scripta Materialia* **108**, 1 (2015).
- [36] M. van Setten, M. Giantomassi, E. Bousquet, M. Verstraete, D. Hamann, X. Gonze, and G.-M. Rignanese, The PseudoDojo: Training and grading a 85 element optimized norm-conserving pseudopotential table, *Comput. Phys. Commun.* **226**, 39 (2018).
- [37] S. R. Xie, Y. Quan, A. C. Hire, B. Deng, J. M. DeStefano, I. Salinas, U. S. Shah, L. Fanfarillo, J. Lim, J. Kim, G. R. Stewart, J. J. Hamlin, P. J. Hirschfeld, and R. G. Hennig, Machine learning of superconducting critical temperature from eliashberg theory, *npj Comput Mater* **8**, 074502 (2022).
- [38] A. Denchfield, H. Park, and R. J. Hemley, Electronic structure of nitrogen-doped lutetium hydrides, *Phys. Rev. Mater.* **8**, L021801 (2024).
- [39] Z. Bai, M. Bhullar, A. Akinpelu, and Y. Yao, Unveiling future superconductors through machine learning, *Materials Today Physics* **43**, 101384 (2024).
- [40] A. Denchfield, H. Park, and R. J. Hemley, Designing multicomponent hydrides with potential high t_c superconductivity (2024), <https://www.pnas.org/doi/pdf/10.1073/pnas.2413096121>.